Received: 29 October 2019 | Accepted: 13 March 2020

DOI: 10.1002/mgg3.1251

ORIGINAL ARTICLE

Molecular Genetics & Genomic Medicine Open Access WILEY

Mutant COMP shapes growth and development of skull and facial structures in mice and humans

Alexander Burger[1] | **Jasmien Roosenboom**[2] | **Mohammad Hossain**[3] | **Seth M. Weinberg**[2,4,5] | **Jacqueline T. Hecht**[1,3] | **Karen L. Posey**[3]

[1]Center for Craniofacial Research, UTHealth School of Dentistry, Houston, TX, USA

[2]Department of Oral Biology, University of Pittsburgh, Pittsburgh, PA, USA

[3]Department of Pediatrics, McGovern Medical School, The University of Texas Health Science Center at Houston (UTHealth), Houston, TX, USA

[4]Department of Human Genetics, University of Pittsburgh, Pittsburgh, PA, USA

[5]Department of Anthropology, University of Pittsburgh, Pittsburgh, PA, USA

Correspondence
Karen L. Posey, Department of Pediatrics, McGovern Medical School at The University of Texas Health Science Center at Houston (UTHealth), Houston, TX, USA.
Email: karen.posey@uth.tmc.edu

Funding information
National Institute of Dental and Craniofacial Research, Grant/Award Number: R01-DE016148 and U01-DE020078; Leah Lewis Family Foundation; National Institutes of Health, Grant/Award Number: R01-AR057117-05

Abstract

Background: Cartilage oligomeric matrix protein (COMP) is an important extracellular matrix protein primarily functioning in the musculoskeletal tissues and especially endochondral bone growth. Mutations in *COMP* cause the skeletal dysplasia pseudoachondroplasia (PSACH) that is characterized by short limbs and fingers, joint laxity, and abnormalities but a striking lack of skull and facial abnormalities.

Methods: This study examined both mice and humans to determine how mutant-COMP affects face and skull growth.

Results: Mutant COMP (MT-COMP) mice were phenotypically distinct. Snout length and skull height were diminished in MT-COMP mouse and the face more closely resembled younger controls. Three-dimensional facial measurements of PSACH faces showed widely spaced eyes, reduced lower facial height, and decreased nasal protrusion, which correlated with a more juvenile appearing face. Neither MT-COMP mice nor PSACH individuals show midface hypoplasia usually associated with abnormal endochondral bone growth. MT-COMP mice do show delayed endochondral and membranous skull ossification that normalizes with age.

Conclusion: Therefore, mutant-COMP affects both endochondral and intramembranous bones of the skull resulting in a reduction of the nose and lower facial height in mice and humans, in addition to its well-defined role in the growth plate chondrocytes.

KEYWORDS

dwarfism, face, mutant cartilage oligomeric matrix protein, pseudoachondroplasia, skull

1 | INTRODUCTION

Pseudoachondroplasia (PSACH) is a well-characterized disproportionate short stature disorder that is caused by mutations in cartilage oligomeric matrix protein (COMP; McKeand, Rotta, & Hecht, 1996; Unger & Hecht, 2001). Pseudoachondroplasia newborns are proportionate, with the disproportionate growth only becoming evident between 18 and 24 months when decelerating overall linear growth is recognized, leading to diagnosis. Rhizomelic shortening of the long bones accompanied by typical radiographic findings are used to make the clinical diagnosis, which can then be confirmed by genetic testing. A striking difference between PSACH and other skeletal dysplasias is the lack

of any discernible facial dysmorphology and normal head circumference (Giordano et al., 1989; Ikegawa et al., 1998; Muensterer, Berdon, Lachman, & Done, 2012). Since mutations in COMP affect endochondral bone formation, the absence of midface hypoplasia is a surprising and unexplained finding.

Previously, we generated and characterized an inducible MT-COMP mouse expressing D469del mutant-COMP in growth plate chondrocytes, which recapitulated the phenotypic features of PSACH (Deere, Sanford, Ferguson, Daniels, & Hecht, 1998; Deere, Sanford, Francomano, Daniels, & Hecht, 1999; Posey et al., 2009, 2012, 2014). Using this model, we showed that misfolded COMP stalls in the ER and participates in premature formation of an extracellular matrix within the ER. Quality control cellular mechanisms are unable to clear the misfolded protein and the massive ER accumulation triggers inflammation and oxidative stresses that severely compromise chondrocyte function, causing chondrocyte death by necroptosis (Hecht et al., 1998, 2004; Merritt, Alcorn, Haynes, & Hecht, 2006; Merritt, Bick, Poindexter, Alcorn, & Hecht, 2007; Posey et al., 2012). Loss of chondrocytes severely impacts endochondral bone growth, thereby diminishing linear growth. Based on these findings, chondrocyte dysfunction should affect midface formation and growth since endochondral bones form several synchondroses within the base of the skull, as well as the nasal septum, which is important for driving anterior growth of the snout (in mice) and nose (in humans). Indeed, gross phenotypic inspection of the MT-COMP mouse skull showed distinct differences in head size and snout (Posey et al., 2014). To better characterize the craniofacial features resulting from COMP mutations, we compared skull measurements obtained from μCT scans of MT-COMP mice and wild-types. We then extended our analysis to humans, comparing three-dimensional (3D)-derived facial measurements between PSACH cases and healthy controls.

2 | MATERIALS AND METHODS

2.1 | Generation of MT-COMP mice

Plasmids containing expression cassettes for mutant D469del-COMP (600,310.0004 OMIM; NM_000095.3sequence) under control of a of tetracycline-inducible (TRE) promoter and recombinant type II collagen driven tetracycline controlled transactivation factor (rtTA) were generated as previously described (Posey et al., 2009). Standard breeding was used to generate bigenic MT-COMP mice in C57BL/6 genetic background. Male MT-COMP and control C57BL/6 mice were administered DOX (500 ng/ml) through the drinking water from birth (through mother's milk) until specific age of analysis. These studies were approved by the Animal Welfare Committee at the McGovern Medical School at The University of Texas Health Science Center at Houston (UT Health).

2.2 | Murine drug administration

Aspirin (0.3 g/l) (Sigma St. Louis, Mo) or resveratrol (0.21 g/l) (Reserveages Organics, Gainesville, FL) was administered in the DOX water from birth to 4 weeks. Dosages of aspirin and resveratrol were based on our previous studies (Posey et al., 2015).

2.3 | μCT scanning

MT-COMP and control C57BL/6 murine skulls were collected at ages 2, 3, 4, 6, 8, and 12 weeks and prepared for μCT scanning (Duke et al., 2009). μCT scans were acquired at room temperature from a minimum of 10 MT-COMP and 10 C57BL/6 mice in each age group at 92 μm isotropic voxel size with an Explore Locus RS μCT (GE Medical Systems, London Ontario). Skull and bone mineral density (BMD) measurements were obtained using MicroView software (GE Healthcare) with a threshold value of 100.

To ensure consistency in BMD measurements, the skulls were aligned so that the temporal-parietal suture was parallel to the x-y plane and the sagittal suture was aligned parallel to the y-z plane. Superior BMD included all bone on cranial vault superior to plane intersecting both temporal-parietal sutures (Figure 3), while inferior BMD included all bone on cranial base inferior to the superior border of the tympanic bulla and posterior to anterior border of tympanic bulla (Figure 3).

Each measurement was made from a set of predefined landmarks, which are shown in Figure 1 and Figure S1. Measurements were as follows: (a) nasal bone—intersection of nasal bones at rostral point to nasal-frontal suture, (b) frontal bone—intersection of frontal bones at nasal-frontal suture to frontal-parietal suture, (c) parietal bone—intersection of parietal bones at frontal-parietal suture to parietal-interparietal suture, (d) interparietal bone—intersection of interparietal bones at parietal-interparietal suture to interparietal-occipital suture, (e) skull height—intersection to interparietal bones at interparietal-occipital suture to anterior portion of foramen magnum, (f) midface width—anterior notch on frontal process lateral to infraorbital fissure, from left to right side (g) frontal width—frontal-squamosal intersection at temporal crest, from left to right side, (h) orbit width—most posterior portion of orbit, left to right side, (i) parietal width—superior aspect of intersection of jugal with zygomatic process of temporal, from left to right side and (j) interparietal width—intersection of parietal, temporal, interparietal bones, from left to right side.

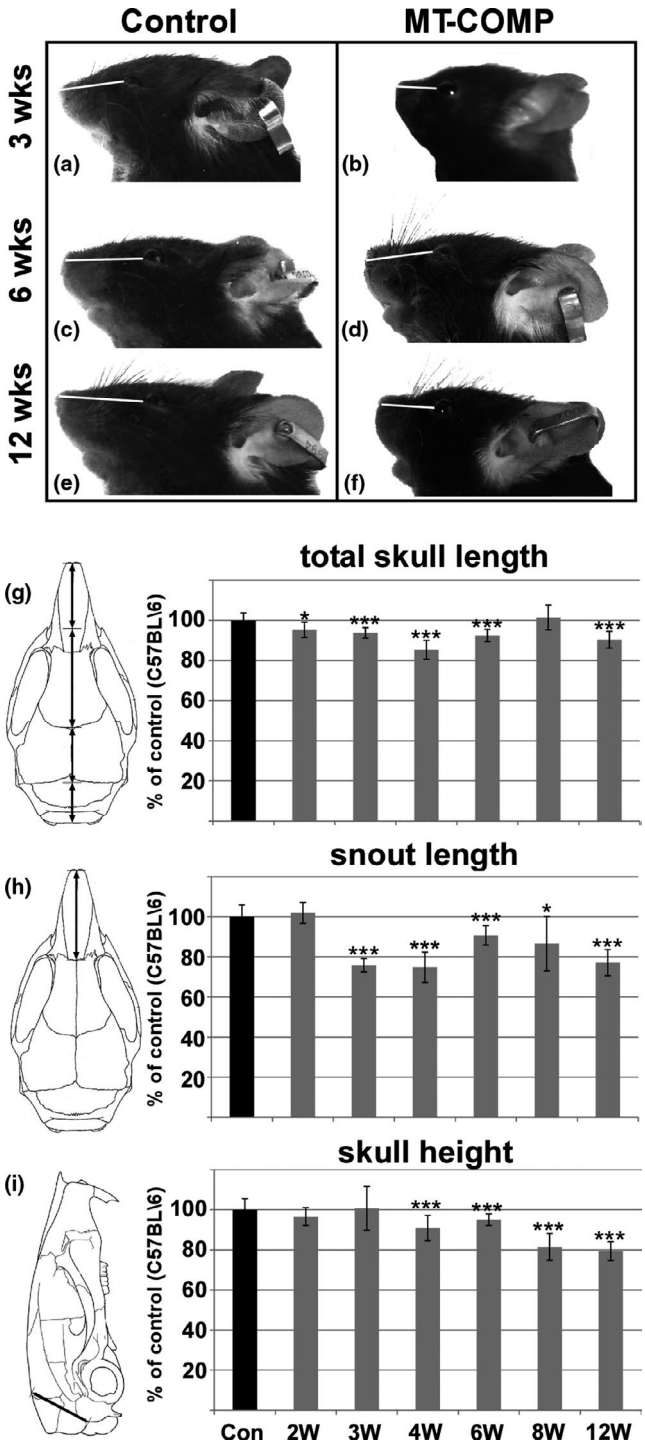

FIGURE 1 Face and skull in MT-COMP mice are smaller. Comparison of MT-COMP (b, d, f) and control (C57BL\6) (a, c, e) mice facial profiles at 3, 6, and 12 weeks. The MT-COMP snout is shorter than controls. Skull measurement in MT-COMP mice from 2 to 12 weeks shows a reduction in total skull length, snout and skull height by 4 week of age (g, h, i). Schematics depicting measurements are shown to the left of measurements. Total skull length (g), snout length (h) and height measurements (i) are shown relative to age matched controls. Con = control C57BL\6 set to 100%, W = weeks and $*p > .05$, $**p > .005$, $***p > .0005$

2.4 | Analysis of mouse skull measurements

Since Shapiro–Wilk test showed a normal distribution for murine skull data, comparisons were performed using an unpaired two-tailed *t* test with the appropriate *t* test given the variance *F*-test outcome. Significance was considered at $*p < .05$; $**p < .01$; $***p < .001$.

2.5 | Recruitment of PSACH and control participants

Nineteen participants with PSACH (11 males, 8 females; average age: range 3–46 years) were recruited at the 2015 and 2017 Little People of America (LPA) annual conventions. The PSACH diagnosis was confirmed by a clinical geneticist (JTH). Ninety controls were selected from the 3D Facial Norms dataset (Weinberg et al., 2016), which consists of over 2,400 craniofacial healthy individuals recruited at four US sites: Pittsburgh, Seattle, Houston, and Iowa City. A minimum of four controls were matched to each PSACH individual. All participants and controls were of Western European descent and had no history of facial birth defects, facial trauma, or facial surgery. All participants provided informed consent prior to recruitment. This study was approved by the Committee for the Protection of Human Subjects UTHealth (HSC-MS-13-0891), the University of Pittsburgh Human Research Protection Office (PRO09060553 and PRO15060396) and the LPA Medical Advisory Board.

2.6 | 3D facial image acquisition and measurement

Three-dimensional facial surface images were collected on PSACH cases with the Vectra H1 (Canfield Scientific, Parsipanny, NJ) portable digital stereophotogrammetry camera system, while the 3dMDface digital stereophotogrammetry camera system (3dMD, Atlanta, GA) was used for controls. Both systems are commercially available, have comparable image quality, and have been independently validated (Aldridge, Boyadjiev, Capone, DeLeon, & Richtsmeier, 2005; Gibelli, Pucciarelli, Cappella, Dolci, & Sforza, 2018) and direct comparison of 3D surface images obtained with these two cameras shows a very high degree of congruence (Camison et al., 2018). Twenty-two standard facial landmarks were collected from each participant's 3D facial image (Figure S3) using 3dMDpatient software for 3dMD images and Vectra VAM software for H1 images. These landmarks were selected to provide sufficient facial coverage and for their high reliability; in tests of observer-related error, these

landmarks have consistently shown intraclass correlations above 0.9(Weinberg et al., 2016). The corresponding x, y, and z coordinates of the 3D landmarks were used to calculate 22 facial linear distances (Figure S3). These distances were defined to be equivalent to standard measurements used in traditional direct anthropometry (Farkas & Deutsch, 1996).

2.7 | Statistical analysis of human facial morphology

ANCOVA was used to compare the mean facial measurements between PSACH cases and controls. Because overall body size can influence facial traits, we included standing height as a covariate in our analyses. Nominal statistical significance was set at $p \leq .05$; the Bonferroni adjusted p value threshold was set at 0.002. All statistical analyses were performed in R (version 1.0.136).

3 | RESULTS

3.1 | MT-COMP reduces skull and snout dimensions

Previously, we showed that mutant-COMP expression reduced skull size and resulted in cartilage persisting for a longer duration in the snout compared to controls (Posey et al., 2012). As shown in Figure 1**,** differences in the size of the face can be appreciated starting at 3 weeks, then remains smaller at 6 and 12 weeks compared to controls. The MT-COMP mice can readily be identified from wild-type litter mates by their facial appearance.

Skull length, width, and height measurements were obtained from μCT images of MT-COMP and control C57BL\6 murine skulls. As shown in Figure 1, MT-COMP skulls were significantly shorter, with reduction in all length parameters. Total length of the MT-COMP skull is reduced beginning at 2 weeks (5%–15%) and snout length is decreased by 3 weeks (15%–24%) (Figure 1g,h). This reduction persisted into adulthood at 12 weeks of age, as growth is minimal after 8–10 weeks of age in mice. The decrease in total skull length is largely attributable to the reduction in snout length. All eye socket measurements were significantly increased in the MT-COMP mice at 4 weeks (Figure 2). There was no reduction skull width measurements (Figure S1).

3.2 | Delayed skull ossification in MT-COMP mice is prevented by aspirin or resveratrol treatments

μCT images of the MT-COMP calvaria, as shown in Figure 3**,** appear "moth-eaten" suggesting an ossification defect. BMD

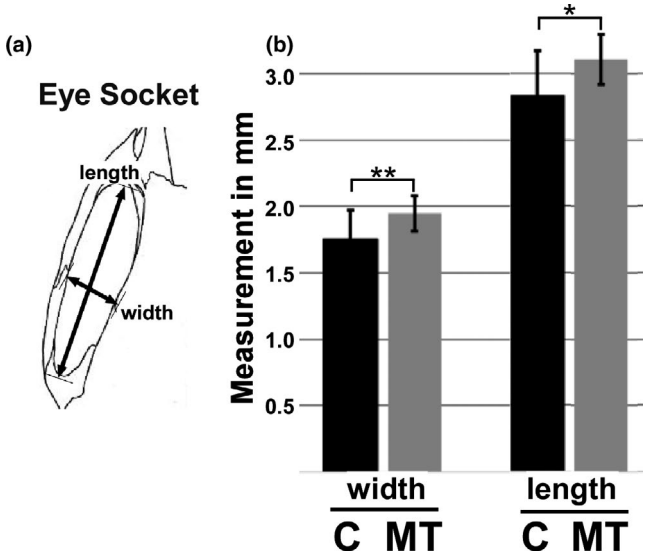

FIGURE 2 MT-COMP murine eye sockets are smaller at 4 weeks. (a) Schematic depicting eye socket measurements. (b) Measurements (mm) are shown relative to age matched controls. MT-COMP eye socket width and lengths are significantly larger. Black bars = control C57BL\6, gray bars = MT-COMP and *$p > .05$, **$p > .005$

measurements of areas of the skull ossified by intramembranous and endochondral processes were greatly reduced (Figure S2). Older mice (≥6 weeks) also had smaller skulls but bone densities were comparable to controls (Figure S2). Based on our previous work demonstrating that aspirin and resveratrol treatments repressed the MT-COMP growth plate pathology (Posey et al., 2015),we asked whether aspirin or resveratrol treatment would affect the skull size and BMD in the MT-COMP mice. Aspirin or resveratrol treatments improved intramembranous and endochondral skull BMD (Figure 3c,d), but had no impact on bone size (data not shown). Neither resveratrol nor aspirin altered control and MT-COMP murine skull size.

3.3 | PSACH faces differ from controls

Fifteen of 22 facial measurements, as shown in Figure 4**,** differed ($p \leq .05$) between the PSACH and control groups with 11 measurements showing differences exceeding Bonferroni adjustment ($p \leq .002$) (Table S1). In PSACH, lower facial height, nasal protrusion, left and right nasal ala length, and labial fissure width were significantly smaller, while inter- and outer canthal width, left and right palpebral fissure length, nasal width, philtrum width and length, upper and lower lip height, and cutaneous lower lip height were significantly larger (Figure 4). Overall facial size (centroid size measured from the 3D landmark configurations after generalized Procrustes alignment) did not differ between PSACH and controls ($p = .64$), suggesting

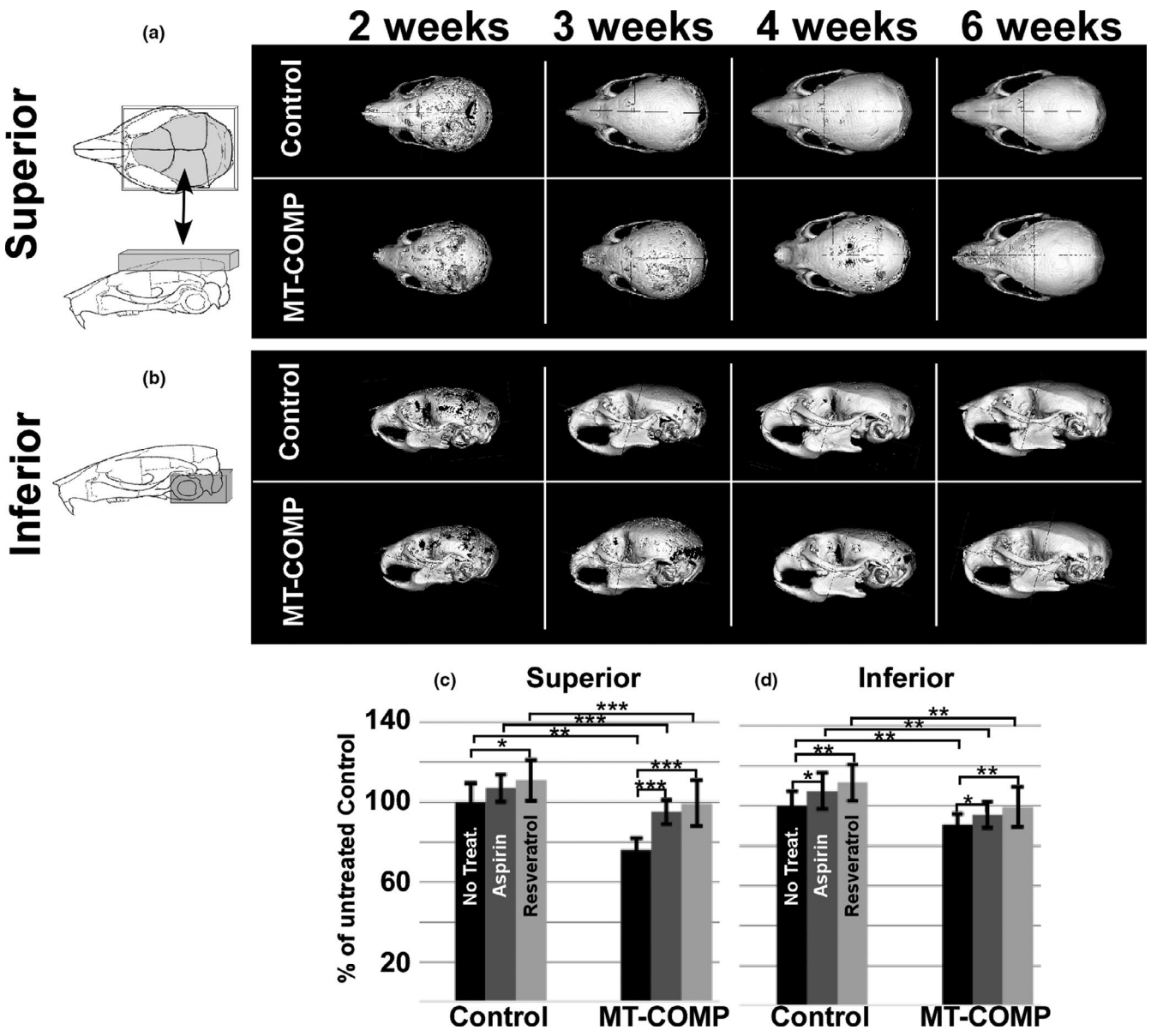

FIGURE 3 Reduced skull ossification is normalized by either aspirin or resveratrol treatments. Superior (a) and inferior (b) views of uCT skull images from control and MT-COMP mice. MT-COMP mouse skulls appear "moth-eaten" at 2, 3 and 4 weeks but are normally ossified by 6 weeks. BMD superior (c) and inferior (d) skull measurements plots (control = black bar and MT-COMP = gray bars) are shown at 4 weeks. Untreated control is set to 100%. In both superior and inferior views, untreated MT-COMP mice show significantly less BMD compared to controls. Both aspirin and resveratrol treatments significantly increased BMD. Treat = treatment; *$p > .05$; **$p > .005$, ***$p > .0005$

that the observed changes in shape are localized and highly specific.

4 | DISCUSSION

It has long been anecdotally reported that individuals with PSACH have an attractive, angular face without dysmorphic features (https://rarediseases.org/rare-diseases/pseudoachondroplasia/). This is surprising given that COMP plays an important role in endochondral bone growth and therefore would be expected to target the cranial base leading to midface hypoplasia. Recognition that MT-COMP mice could be identified grossly by a reduced snout, led to quantification of skull measurements in the MT-COMP mice and facial features in PSACH cases. Both MT-COMP mice and PSACH cases showed reduced lower face and nasal dimensions, retaining a somewhat juvenile appearance into adulthood (Figures 1, 4 and 5 and Table S1).

Figure 5 shows that the snout of MT-COMP mice is reduced compared to wild-type controls, resulting in the retention of a juvenile appearance. The MT-COMP mouse at 3 weeks of age is more similar to wild-type controls at 2 weeks than the wild-type controls at 3 weeks. In comparison, the

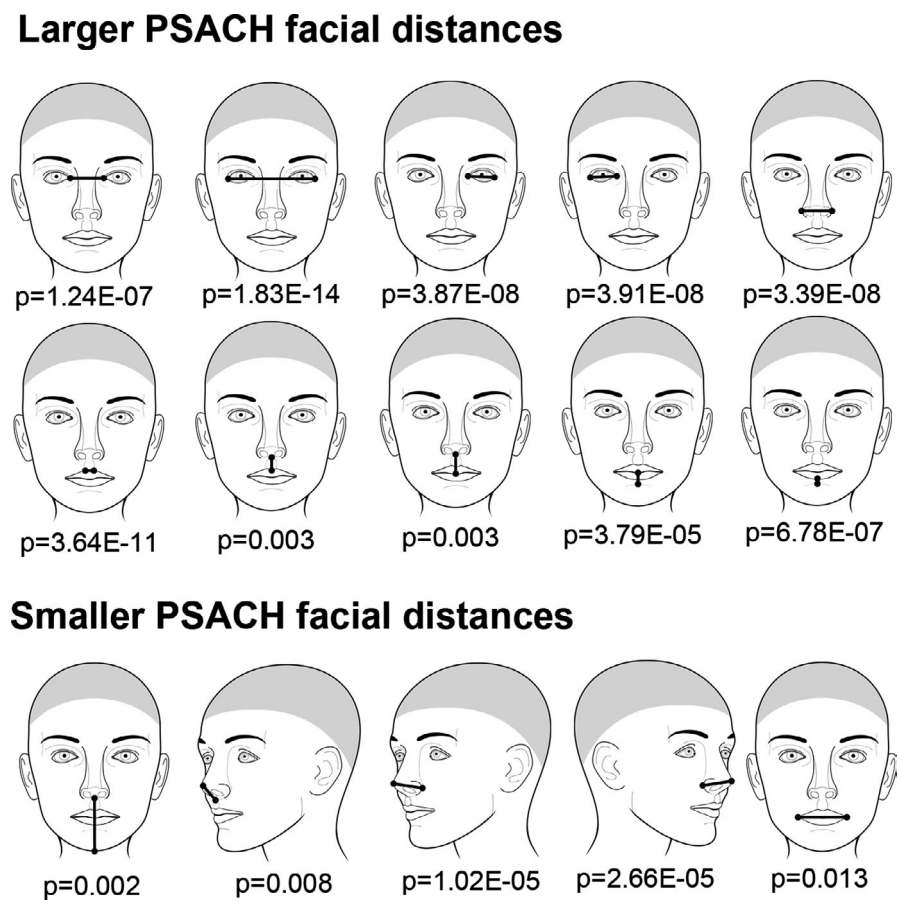

FIGURE 4 Anthropometric measurements that differ in PSACH faces. A total of 15 facial measurements were significantly different in pseudoachondroplasia cases compared with matched controls ($p \leq .05$). Ten facial distances were larger and five distances smaller in pseudoachondroplasia cases compared with matched controls, even after controlling for body size. Of the 15 measurements, 11 remained statistically significant after adjusting for multiple comparisons ($p \leq .002$). See Table S1 for details

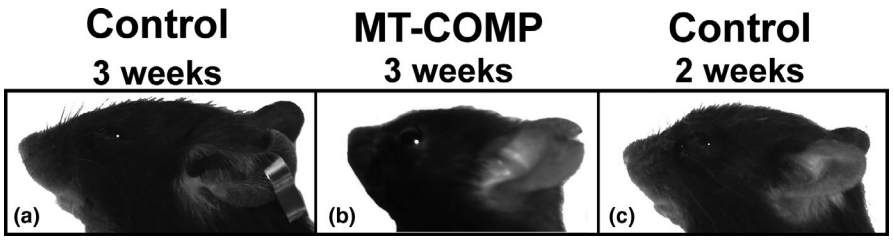

FIGURE 5 MT-COMP face compared to control mice at different ages. MT-COMP mice at 3 weeks of age more closely resemble younger controls than age matched control

human facial analysis showed that individuals with PSACH have a reduced lower facial height, reduced nasal protrusion and more widely spaced eyes. Even though all of these changes are within the normal range of facial variation, these characteristics are associated with a more juvenile facial appearance (Ferrario, Sforza, Serrao, Ciusa, & Dellavia, 2003). While comparison of murine and human faces is not straightforward, some findings are consistent including PSACH lower facial height and reduced nasal protrusion that correspond to smaller MT-COMP snout length and skull height. Several of these facial differences are consistent with changes in the cranial base. The mild hypertelorism in PSACH cases, for example, may be related to change in the growth of bones comprising the anterior cranial base (Moss, 1965; Tessier, 1972). The reduced snout length (in mice) and reduced nasal protrusion may be related to changes in the cartilaginous nasal septum, which has a major impact on the early anterior growth of the midface (Delaire & Precious, 1986)

In addition to altering facial features, mutant-COMP affects murine skull BMD by temporarily delaying ossification between 3 and 4 weeks. This is similar to that observed in the murine MT-COMP long bones, which showed lower BMD particularly in the ends of the bones (Coustry et al., 2018; Hecht et al., 1995; Posey et al., 2009). Interestingly and unexpected, intramembranous bone ossification was also delayed. The underossified calvaria is difficult to explain given that mutant-COMP expression is restricted to tissues that express type II collagen. The calvaria ossifies through intramembranous ossification and does not involve calcification of cartilage (type II collagen tissue; Breeland & Menezes, 2019). Mutant-COMP expression had the greatest impact on "adolescent" mice (3 and 4 weeks),

while in younger mice, the skulls were smaller and BMD was reduced. By6 weeks, skulls remained smaller but BMD was comparable to controls (Figure S2). These findings suggest that mutant-COMP causes a temporary delay in ossification of both membranous and endochondral bones of the skull.

Previously, we showed that aspirin or resveratrol treatment partially rescued long bone length in MT-COMP mice (Posey et al., 2015). Interestingly, while these treatments did not normalize skull size, ossification was improved. Both aspirin and resveratrol increased inferior BMD, while only resveratrol increased superior BMD in both control and MT-COMP mice. The improvement by resveratrol of both inferior and superior skull BMD is similar to its superior performance in dampening the MT-COMP growth plate chondrocyte pathology (Posey et al., 2015).

The novel results of this study characterize and quantify the unique facial features in PSACH not previously appreciated and, to some degree, recapitulated in MT-COMP mice. Mutant-COMP affects facial and skull development in mice and humans in distinct patterns resulting in a more juvenile appearance, which may account for previous anecdotal reports of heighted facial attractiveness. Additional studies are needed to better understand the mutant-COMP molecular mechanisms underlying these differences in skull and face, which are distinct from the long bone pathology.

ACKNOWLEDGMENTS

This work was supported by the National Institute of Arthritis and Musculoskeletal and Skin Diseases of the National Institutes of Health [R01-AR057117-05] (JTH and KLP), the National Institute of Dental and Craniofacial Research [U01-DE020078 and R01-DE016148] (SMW), and The Leah Lewis Family Foundation. The content is solely the responsibility of the authors and does not necessarily represent the official views of the National Institutes of Health or the National Science Foundation. These funding bodies had no role in the design, collection, analysis, and interpretation of data, in the writing of the manuscript, or in the decision to submit the manuscript for publication.

CONFLICT OF INTEREST

There are no conflict of interest to disclose.

AUTHORS' CONTRIBUTIONS

Alexander Burger collected the mouse skull data. Jasmien Roosenboom collected 3D photos, analyzed human data, and contributed to manuscript preparation. Mohammad Hossain collected the mouse skull data. Seth M. Weinberg analyzed human data, contributed to manuscript preparation, and project management. Jacqueline T. Hecht collected 3D photos, contributed to manuscript preparation and project management. Karen L. Posey collected 3D photos, analyzed mouse data, contributed to manuscript preparation, and project management.

DATA AVAILABILITY STATEMENT

Data from the controls used in this paper were obtained from the 3D Facial Norms Project, which is freely available through the FaceBase Consortium (www.facebase.org).

ORCID

Karen L. Posey https://orcid.org/0000-0003-1234-6087

REFERENCES

Aldridge, K., Boyadjiev, S. A., Capone, G. T., DeLeon, V. B., & Richtsmeier, J. T. (2005). Precision and error of three-dimensional phenotypic measures acquired from 3dMD photogrammetric images. *American Journal of Medical Genetics. Part A*, *138A*(3), 247–253. https://doi.org/10.1002/ajmg.a.30959

Breeland, G., & Menezes, R. G. (2019). *Embryology, bone ossification*. Treasure Island, FL: StatPearls.

Camison, L., Bykowski, M., Lee, W. W., Carlson, J. C., Roosenboom, J., Goldstein, J. A., … Weinberg, S. M. (2018). Validation of the Vectra H1 portable three-dimensional photogrammetry system for facial imaging. *International Journal of Oral and Maxillofacial Surgery*, *47*(3), 403–410. https://doi.org/10.1016/j.ijom.2017.08.008

Coustry, F., Posey, K. L., Maerz, T., Baker, K., Abraham, A. M., Ambrose, C. G., … Hecht, J. T. (2018). Mutant cartilage oligomeric matrix cartilage (COMP) compromises bone integrity, joint function and the balance between adipogenesis and osteogenesis. *Matrix Biology*, *67*, 75–89. https://doi.org/10.1016/j.matbio.2017.12.014

Deere, M., Sanford, T., Ferguson, H. L., Daniels, K., & Hecht, J. T. (1998). Identification of twelve mutations in cartilage oligomeric matrix protein (COMP) in patients with pseudoachondroplasia. *American Journal of Medical Genetics*, *80*(5), 510–513. https://doi.org/10.1002/(SICI)1096-8628(19981228)80:5<510:AID-AJMG14>3.0.CO;2-F

Deere, M., Sanford, T., Francomano, C. A., Daniels, K., & Hecht, J. T. (1999). Identification of nine novel mutations in cartilage oligomeric matrix protein in patients with pseudoachondroplasia and multiple epiphyseal dysplasia. *American Journal of Medical Genetics*, *85*(5), 486–490. Retrieved from http://www.ncbi.nlm.nih.gov/entrez/query.fcgi?cmd=Retrieve&db=PubMed&dopt=Citation&list_uids=10405447

Delaire, J., & Precious, D. (1986). Influence of the nasal septum on maxillonasal growth in patients with congenital labiomaxillary cleft. *Cleft Palate J*, *23*(4), 270–277. Retrieved from https://www.ncbi.nlm.nih.gov/pubmed/3464365

Duke, P. J., Doan, L., Luong, H., Kelley, C., Leboeuf, W., Diep, Q., … Cody, D. D. (2009). Correlation between micro-Ct sections and histological sections of mouse skull defects implanted with engineered cartilage. *Gravitational and Space Biology Bulletin*, *22*(2), 45–50. Retrieved from https://www.ncbi.nlm.nih.gov/pubmed/24478573

Farkas, L. G., & Deutsch, C. K. (1996). Anthropometric determination of craniofacial morphology. *American Journal of Medical Genetics*, *65*(1), 1–4. https://doi.org/10.1002/ajmg.1320650102

Ferrario, V. F., Sforza, C., Serrao, G., Ciusa, V., & Dellavia, C. (2003). Growth and aging of facial soft tissues: A computerized three-dimensional mesh diagram analysis. *Clinical Anatomy*, *16*(5), 420–433. https://doi.org/10.1002/ca.10154

Gibelli, D., Pucciarelli, V., Cappella, A., Dolci, C., & Sforza, C. (2018). Are portable stereophotogrammetric devices reliable in facial imaging? A validation study of VECTRA H1 device. *Journal of Oral and Maxillofacial Surgery*, *76*(8), 1772–1784. https://doi.org/10.1016/j.joms.2018.01.021

Giordano, F., Corso, D., Basile, G., Noto, D., Orsi, E., Chiappara, G. M., & Camera, G. (1989). Pseudoachondrodysplasia (pseudoachondroplastic spondyloepiphyseal dysplasia). Description of 2 non-familial cases. *Pathologica*, *81*(1076), 627–634. Retrieved from http://www.ncbi.nlm.nih.gov/pubmed/2635292

Hecht, J. T., Makitie, O., Hayes, E., Haynes, R., Susic, M., Montufar-Solis, D., … Cole, W. G. (2004). Chondrocyte cell death and intracellular distribution of COMP and type IX collagen in the pseudoachondroplasia growth plate. *Journal of Orthopaedic Research*, *22*(4), 759–767. https://doi.org/10.1016/j.orthres.2003.11.010

Hecht, J. T., Montufar-Solis, D., Decker, G., Lawler, J., Daniels, K., & Duke, P. J. (1998). Retention of cartilage oligomeric matrix protein (COMP) and cell death in redifferentiated pseudoachondroplasia chondrocytes. *Matrix Biology*, *17*(8–9), 625–633. Retrieved from http://www.ncbi.nlm.nih.gov/entrez/query.fcgi?cmd=Retrieve&db=PubMed&dopt=Citation&list_uids=9923655

Hecht, J. T., Nelson, L. D., Crowder, E., Wang, Y., Elder, F. F. B., Harrison, W. R., … Lawler, J. (1995). Mutations in exon 17B of cartilage oligomeric matrix protein (COMP) cause pseudoachondroplasia. *Nature Genetics*, *10*(3), 325–329. https://doi.org/10.1038/ng0795-325

Ikegawa, S., Ohashi, H., Hosoda, F., Fukushima, Y., Ohki, M., & Nakamura, Y. (1998). Pseudoachondroplasia with de novo deletion [del(11)(q21q22.2)]. *American Journal of Medical Genetics*, *77*(5), 356–359. Retrieved from http://www.ncbi.nlm.nih.gov/entrez/query.fcgi?cmd=Retrieve&db=PubMed&dopt=Citation&list_uids=9632164

McKeand, J., Rotta, J., & Hecht, J. T. (1996). Natural history study of pseudoachondroplasia. *American Journal of Medical Genetics*, *63*(2), 406–410. https://doi.org/10.1002/(SICI)1096-8628(19960517)63:2<406:AID-AJMG16>3.0.CO;2-O

Merritt, T. M., Alcorn, J. L., Haynes, R., & Hecht, J. T. (2006). Expression of mutant cartilage oligomeric matrix protein in human chondrocytes induces the pseudoachondroplasia phenotype. *Journal of Orthopaedic Research*, *24*(4), 700–707. Retrieved from http://www.ncbi.nlm.nih.gov/entrez/query.fcgi?cmd=Retrieve&db=-PubMed&dopt=Citation&list_uids=16514635

Merritt, T. M., Bick, R., Poindexter, B. J., Alcorn, J. L., & Hecht, J. T. (2007). Unique matrix structure in the rough endoplasmic reticulum cisternae of pseudoachondroplasia chondrocytes. *American Journal of Pathology*, *170*(1), 293–300. Retrieved from http://www.ncbi.nlm.nih.gov/entrez/query.fcgi?cmd=Retrieve&db=PubMed&dopt=Citation&list_uids=17200202

Moss, M. L. (1965). Hypertelorism and cleft palate deformity. *Acta Anat (Basel)*, *61*(4), 547–557. https://doi.org/10.1159/000142714

Muensterer, O. J., Berdon, W. E., Lachman, R. S., & Done, S. L. (2012). Pseudoachondroplasia and the seven Ovitz siblings who survived Auschwitz. *Pediatric Radiology*, *42*(4), 475–480. https://doi.org/10.1007/s00247-012-2364-8

Posey, K. L., Coustry, F., Veerisetty, A. C., Hossain, M., Alcorn, J. L., & Hecht, J. T. (2015). Antioxidant and anti-inflammatory agents mitigate pathology in a mouse model of pseudoachondroplasia. *Human Molecular Genetics*, *24*(14), 3918–3928. https://doi.org/10.1093/hmg/ddv122

Posey, K. L., Coustry, F., Veerisetty, A. C., Liu, P., Alcorn, J. L., & Hecht, J. T. (2012). Chop (Ddit3) is essential for D469del-COMP retention and cell death in chondrocytes in an inducible transgenic mouse model of pseudoachondroplasia. *American Journal of Pathology*, *180*(2), 727–737. https://doi.org/10.1016/j.ajpath.2011.10.035

Posey, K. L., Coustry, F., Veerisetty, A. C., Liu, P., Alcorn, J. L., & Hecht, J. T. (2014). Chondrocyte-specific pathology during skeletal growth and therapeutics in a murine model of pseudoachondroplasia. *Journal of Bone and Mineral Research*, *29*(5), 1258–1268. https://doi.org/10.1002/jbmr.2139

Posey, K. L., Veerisetty, A. C., Liu, P., Wang, H. R., Poindexter, B. J., Bick, R., … Hecht, J. T. (2009). An inducible cartilage oligomeric matrix protein mouse model recapitulates human pseudoachondroplasia phenotype. *The American Journal of Pathology*, *175*(4), 1555–1563. https://doi.org/10.2353/ajpath.2009.090184

Tessier, P. (1972). Orbital hypertelorism. I. Successive surgical attempts. Material and methods. Causes and mechanisms. *Scandinavian Journal of Plastic and Reconstructive Surgery*, *6*(2), 135–155. Retrieved from https://www.ncbi.nlm.nih.gov/pubmed/4652235

Unger, S., & Hecht, J. T. (2001). Pseudoachondroplasia and multiple epiphyseal dysplasia: New etiologic developments. *American Journal of Medical Genetics*, *106*(4), 244–250. Retrieved from http://www.ncbi.nlm.nih.gov/entrez/query.fcgi?cmd=Retrieve&db=PubMed&dopt=Citation&list_uids=11891674

Weinberg, S. M., Raffensperger, Z. D., Kesterke, M. J., Heike, C. L., Cunningham, M. L., Hecht, J. T., … Marazita, M. L. (2016). The 3D facial norms database: Part 1. A web-based craniofacial anthropometric and image repository for the clinical and research community. *Cleft Palate-Craniofacial Journal*, *53*(6), e185–e197. https://doi.org/10.1597/15-199

SUPPORTING INFORMATION

Additional supporting information may be found online in the Supporting Information section.

How to cite this article: Burger A, Roosenboom J, Hossain M, Weinberg SM, Hecht JT, Posey KL. Mutant COMP shapes growth and development of skull and facial structures in mice and humans. *Mol Genet Genomic Med*. 2020;8:e1251. https://doi.org/10.1002/mgg3.1251